



HAL
open science

Synchrony in Excitatory Neural Networks

David Hansel, Germán Mato, Claude Meunier

► **To cite this version:**

David Hansel, Germán Mato, Claude Meunier. Synchrony in Excitatory Neural Networks. *Neural Computation*, 1995, 7 (2), pp.307-337. 10.1162/neco.1995.7.2.307 . hal-02383930

HAL Id: hal-02383930

<https://hal.science/hal-02383930>

Submitted on 15 Mar 2024

HAL is a multi-disciplinary open access archive for the deposit and dissemination of scientific research documents, whether they are published or not. The documents may come from teaching and research institutions in France or abroad, or from public or private research centers.

L'archive ouverte pluridisciplinaire **HAL**, est destinée au dépôt et à la diffusion de documents scientifiques de niveau recherche, publiés ou non, émanant des établissements d'enseignement et de recherche français ou étrangers, des laboratoires publics ou privés.

Synchrony in Excitatory Neural Networks

D. Hansel

*Centre de Physique Théorique UPR014 CNRS, Ecole Polytechnique, 91128 Palaiseau
Cedex, France*

G. Mato

*Racah Institute of Physics and Center for Neural Computation, Hebrew University,
91904 Jerusalem, Israel*

C. Meunier

*Centre de Physique Théorique UPR014 CNRS, Ecole Polytechnique, 91128 Palaiseau
Cedex, France*

Synchronization properties of fully connected networks of identical oscillatory neurons are studied, assuming purely excitatory interactions. We analyze their dependence on the time course of the synaptic interaction and on the response of the neurons to small depolarizations. Two types of responses are distinguished. In the first type, neurons always respond to small depolarization by advancing the next spike. In the second type, an excitatory postsynaptic potential (EPSP) received after the refractory period delays the firing of the next spike, while an EPSP received at a later time advances the firing. For these two types of responses we derive general conditions under which excitation destabilizes in-phase synchrony. We show that excitation is generally desynchronizing for neurons with a response of type I but can be synchronizing for responses of type II when the synaptic interactions are fast. These results are illustrated on three models of neurons: the Lapicque integrate-and-fire model, the model of Connor *et al.*, and the Hodgkin–Huxley model. The latter exhibits a type II response, at variance with the first two models, that have type I responses. We then examine the consequences of these results for large networks, focusing on the states of partial coherence that emerge. Finally, we study the Lapicque model and the model of Connor *et al.* at large coupling and show that excitation can be desynchronizing even beyond the weak coupling regime.

1 Introduction

Synaptic interactions between neurons are usually classified as excitatory or inhibitory according to the value of the reversal potential of the

synapses. However, as observed in Kopell (1988), there is no obvious relationship between this classification and the dynamic behavior of a network of interconnected neurons. If one focuses on synchronization properties of neural systems, a more fundamental classification of the interactions should be in terms of “synchronizing interactions,” that favor a stable in-phase state (where all the neurons fire at the same time) and “desynchronizing interactions” that tend to destabilize this state.

This paper examines the conditions under which excitatory interactions synchronize a network of neurons that fire spikes periodically. In particular, we will relate the synchronization properties to the response of the neurons to perturbations of their membrane potential. For this purpose we focus on a simple case: a homogeneous and fully connected network of excitatory neurons. Moreover we do not take into account interaction delays. Some of the results presented in this paper have been reported in Hansel *et al.* (1993c).

In many cases a small excitatory postsynaptic potential (EPSP) systematically advances the next spike of the neuron, except when it occurs during the period of refractoriness where it has no effect. As shown below, this form of response is found, for instance, in simple integrate-and-fire models and in the model of Connor *et al.* (1977). We call such a response to EPSPs a response of type I. Using the phase reduction method (Ermentrout and Kopell 1991; Kuramoto 1984; Neu 1979), a powerful technique that has been applied recently to neural modeling (Ermentrout and Kopell 1991; Grannan *et al.* 1992; Hansel *et al.* 1993a,c; Kopell 1988), we show that in general two weakly coupled neurons with a response of type I do not lock stably in-phase. We then illustrate this desynchronizing effect of excitation on specific models of neurons and show that it occurs for synapses with physiologically relevant time constants (for non-NMDA synapses).

If the in-phase state of a pair of neurons is unstable, a network of such neurons cannot synchronize fully. Partially coherent states then emerge in the network. It is even possible that no coherence can be achieved and that the asynchronous state turns out to be stable. We give examples of such collective states of large networks, focusing on the model of Connor *et al.*, which exhibits “rotating waves” (Kuramoto 1991; Watanabe and Strogatz 1993) and switching states (Hansel *et al.* 1993b). Our study is based on numerical simulations, but it should be noted that some properties of these states can be studied analytically in the framework of phase reduction (Kuramoto 1984; Monnet *et al.* 1994; Watanabe and Strogatz 1993).

Beyond the weak coupling limit, our general arguments on the desynchronizing nature of excitation for neurons of type I no longer hold and our investigation relies on the study of specific models: namely an integrate-and-fire model and the model of Connor *et al.* For both models we find that in an intermediate (but wide) range of coupling strength the predictions of phase reduction remain qualitatively valid. However, for

stronger coupling, the deviations from this limit become important. For the integrate-and-fire model we show analytically that the desynchronizing effect of the excitation is amplified at strong coupling, anti-phase locking being achieved even at finite coupling. For the model of Connor *et al.* our simulations show that if the rise time of the interaction is large enough the situation is very similar to what is found for the integrate-and-fire model. On the other hand, for a short rise time, increasing the coupling strength can make the excitation *synchronizing*.

Not all the neurons have a response of type I. Another form of response is found, for instance, for the standard Hodgkin–Huxley (HH) model (Hodgkin and Huxley 1952). There is a region of the limit cycle, just after the refractory period, where a depolarization delays the firing of the next spike (for reasons that will become clear later, we will say that in this region the response is negative). A response of this kind will be called type II. We show that at weak coupling the region of negative response tends to stabilize the in-phase state. The Hodgkin–Huxley model provides an example in which this stabilizing effect is strong enough to make fast excitatory interactions synchronizing. For slower interactions excitation is once again desynchronizing.

The paper is organized as follows. In Section 2 we present the basic types of models of neurons considered in this study. After recalling the phase reduction method our general results at weak coupling are established and illustrated on specific examples in Section 3. In Section 4 the case of large coupling is addressed. Finally, the last section is devoted to a discussion.

2 The Models

2.1 Conductance-Based Neurons. Conductance-based models account for spiking by incorporating the dynamics of voltage-dependent membrane currents (see for instance Tuckwell 1988). In this framework, the dynamics of a neuron is described by the equation for the membrane potential V :

$$C \frac{dV}{dt} = I_{\text{ext}} - \sum_i g_i(X_i)(V - V_i) + I_{\text{syn}}(t) \quad (2.1)$$

where C is the membrane capacitance, and g_i and V_i are, respectively, the voltage-dependent conductance of the i th ionic current and its reversal potential. The gating variables of the i th current have been denoted here by X_i and the model must also specify their relaxation dynamics. The synaptic current $I_{\text{syn}}(t)$ is modeled as

$$I_{\text{syn}}(t) = -(V - V_{\text{syn}})g_{\text{syn}}(t) \quad (2.2)$$

where V_{syn} is the reversal potential of the synapse, and

$$g_{\text{syn}}(t) = g \sum_{\text{spikes}} f(t - t_{\text{spike}}), \quad (2.3)$$

the summation being performed over all the spikes emitted by the presynaptic neurons at times t_{spike} . The synaptic interaction is usually classified according to whether V_{syn} is larger or smaller than the threshold potential V_{th} , at which the postsynaptic neuron generates spikes. For $V_{\text{syn}} > V_{\text{th}}$ the interaction is called excitatory, while for $V_{\text{syn}} < V_{\text{th}}$ it is called inhibitory. The function f is normalized so that its peak value is 1; g is then the maximal synaptic conductance induced by a postsynaptic potential.

Several forms can be used for the function $f(t)$. A standard choice is

$$f(t) = A \left(\exp \left[-\frac{t}{\tau_1} \right] - \exp \left[-\frac{t}{\tau_2} \right] \right) \quad (2.4)$$

The function f is maximum at the peak time $t_p = [\tau_1 \tau_2 / (\tau_1 - \tau_2)] \log(\tau_1 / \tau_2)$ and the constant of normalization A then reads:

$$A = \frac{1}{\exp[-t_p/\tau_1] - \exp[-t_p/\tau_2]} \quad (2.5)$$

The characteristic times τ_1 and τ_2 are, respectively, the decay and rise times of the synapse. When $\tau_1 = \tau_2 = \tau$ one obtains the so-called ‘‘alpha function’’:

$$f(t) = \frac{et}{\tau} \exp \left[-\frac{t}{\tau} \right] \quad (2.6)$$

Two well-known conductance-based models considered in this work are the Hodgkin–Huxley model and the model of Connor *et al.* The former was introduced to account for spike generation in the squid axon and relies on two voltage-dependent currents: the sodium current and the delayed rectifier potassium current (Hodgkin and Huxley 1952). The latter also incorporates an A-current and was introduced to conform to voltage-clamp data from repetitive walking leg axons of a crustacean (Connor *et al.* 1977). This A-current was subsequently found in many types of neurons (Rogawski 1985). Details on these models are given in the appendix.

2.2 Integrate-and-Fire Neurons. Another class of models commonly used in neural modeling are integrate-and-fire models (Tuckwell 1988). These models do not rely on a biophysical description of firing and their simplicity makes them more easily amenable to analytical studies than conductance-based models (Abbott and van Vreeswijk 1993; Treves 1993; Tsodyks *et al.* 1993).

In the simplest integrate-and-fire model, the Lapicque model, the membrane potential of a neuron satisfies the differential equation:

$$\frac{dV}{dt} = -\frac{V}{\tau_0} + I_{\text{ext}} + I_{\text{syn}}(t) \quad (2.7)$$

for $0 < V < \theta$ and

$$V(t_0^+) = 0 \quad \text{if} \quad V(t_0^-) = \theta \quad (2.8)$$

This last condition corresponds to a fast resetting of the neuron after the firing of a spike at time t_0 ; this firing occurs when the membrane potential reaches the spiking threshold θ . The time constant of the membrane is τ_0 and I_{ext} is a bias current that determines the firing rate of the neuron. The last term in equation 2.1 is the synaptic current received by the neuron. For this model we adopt

$$I_{\text{syn}}(t) = g \sum_{\text{spikes}} f(t - t_{\text{spike}}) \quad (2.9)$$

where the function $f(t)$ is given by equation 2.4 and the summation is done over all the spikes emitted prior to t by all the neurons presynaptic to the neuron we consider. This simple form of synaptic interaction is justified as a first approximation for excitatory interactions ($g > 0$) as no description of the spike is incorporated in the model and the driving force $V_{\text{syn}} - V$ remains approximately constant in the subthreshold regime. Note that the membrane capacitance C was assumed to equal 1 and omitted from 2.7.

One can also introduce in this model a refractory period, if necessary, by imposing that $V(t)$ remains equal to 0 for a time T_r after the firing of a spike. If the neurons are not interacting ($g = 0$) they emit spikes periodically with a period $T_0 = T_r - \tau_0 \ln(1 - \theta/I_{\text{ext}})$, for $I_{\text{ext}} > \theta$. Without loss of generality one can assume $\tau_0 = 1$, measuring then the time in units of τ_0 .

3 The Case of Weak Interaction

3.1 Reduction to Phase Models. In general, the dynamic equations of conductance-based neurons cannot be solved analytically and the study of synchronization in networks of such neurons must rely on numerical computations. However, if the neurons display a periodic behavior (limit cycle), if their firing rates all lie in a narrow range, and if the coupling is weak, a reduction to a phase model can be performed that greatly simplifies the analysis.

Let us briefly recall the principle of such a reduction (Ermentrout and Kopell 1991; Kopell 1988; Kuramoto 1984). It is based on an averaging theorem that enables one to describe the state of each neuron i by a phase variable ψ_i ($i = 1, \dots, N$, where N is the number of nonlinear cycle oscillators in the system) indicating the position of neuron i on its limit cycle and to replace the original system of equations for the N oscillators by a simpler set of N differential equations that governs the time evolution of the N coupled phase variables. This differential systems reads

$$\frac{d\psi_i}{dt} = \omega_i + \sum_{j \neq i} \Gamma(\psi_i - \psi_j) \quad (3.1)$$

where ω_i is the natural frequency of neuron i , that is, its frequency at zero coupling, while Γ gives the effective interaction between any two neurons. Γ depends only on the relative phase on the two neurons. The system is invariant with respect to a global rotation of all the phases, that are thus defined up to an arbitrary constant. It is conventional to choose the phases so that firing occurs for $\psi_i = 0 \bmod 2\pi$. Note that the dependence on the relative phases stems from the assumption of weak coupling. For phase models at arbitrary coupling the interaction between two neurons depends on the values of both phases; the integrate-and-fire model studied below provides an example of that situation.

The effective interaction between the phases is given by

$$\Gamma(\psi_i - \psi_j) = \frac{1}{2\pi} \int_0^{2\pi} Z(u + \psi_i) I_{\text{syn}}(u + \psi_i, u + \psi_j) du \quad (3.2)$$

This formula can be interpreted as follows. The effective interaction between the presynaptic neuron j and the postsynaptic neuron i is obtained by convolving over one period the synaptic current $I_{\text{syn}}(\psi_i, \psi_j)$, due to the EPSPs (or IPSPs) generated by neuron j , and the "response function" Z of the target neuron i to these perturbations. The function Z is nothing else than the phase resetting curve of the neuron in the limit of vanishingly small perturbations of the membrane potential. If $Z(\psi) > 0$ a small and instantaneous depolarization at ψ of the neuron will advance the next spike; if $Z(\psi) < 0$ the next spike will be delayed. To calculate Γ one must implement numerically the rigorous method described in Ermentrout and Kopell (1984) and Kopell (1988) or the more qualitative algorithm explained in Hansel *et al.* (1993a). Note that the 2π -periodic function Γ depends only on the single neuron dynamics. Once this effective phase interaction is determined it can be used to analyze networks of arbitrary complexity. Note also that the introduction of a delay Δ in the interaction is immediate in this formalism: $\Gamma(\psi)$ is just replaced by $\Gamma(\psi - \Delta)$.

The synaptic current in 3.2 is

$$I_{\text{syn}}(\phi, \psi) = -g_{\text{syn}}(\psi)[V(\phi) - V_{\text{syn}}] \quad (3.3)$$

for an interaction described by equation 2.2 and

$$I_{\text{syn}}(\phi, \psi) = g_{\text{syn}}(\psi) \quad (3.4)$$

for an interaction described by a current independent of the postsynaptic voltage as in the integrate-and-fire model of Section 2.2. In the two cases the function $g_{\text{syn}}(\psi)$ must take into account all the spikes emitted by the presynaptic neuron and has to be computed at the leading order in g . It has period 2π and is defined, for $0 \leq u < 2\pi$, by

$$g_{\text{syn}}(u) = gA \left(\frac{e^{-u/\psi_1}}{1 - e^{-2\pi/\psi_1}} - \frac{e^{-u/\psi_2}}{1 - e^{-2\pi/\psi_2}} \right) \quad (3.5)$$

where we have set $\psi_1 = 2\pi\tau_1/T$ and $\psi_2 = 2\pi\tau_2/T$. As all the spikes are taken into account the maximum is displaced with respect to the maximum of f and is given by

$$\psi_p = \frac{\psi_1\psi_2}{\psi_1 - \psi_2} \log \left[\frac{\psi_1(1 - e^{-2\pi/\psi_1})}{\psi_2(1 - e^{-2\pi/\psi_2})} \right] \quad (3.6)$$

This quantity is an increasing function of ψ_1 and ψ_2 and remains bounded: $\psi_p \leq \pi$. The peak of the interaction thus always occurs within the first half of the firing period and the limiting value, π , is reached for infinitely large τ_1 and τ_2 .

The reduction to phases is exact only for small frequency dispersion:

$$\frac{\omega_i - \bar{\omega}}{\bar{\omega}} \ll 1 \quad (3.7)$$

where $\bar{\omega}$ is the average frequency of the neural population. Another condition is that the coupling should be weak enough for averaging to be valid. This condition reads:

$$\epsilon = \frac{g}{\bar{\omega}} \ll 1 \quad (3.8)$$

The predictions of the phase model are then accurate at leading order in ϵ and over times of the order of $1/\epsilon$. In addition, phase reduction assumes that the coupling is small enough for amplitude effects to be neglected. The more stable the limit cycle the weaker this constraint will be, but it is difficult to derive quantitative a priori estimates of the validity of the phase reduction. However, predictions of phase models often remain valid, at least qualitatively, for moderate values of the coupling. This will be the case for the examples studied below.

3.2 A Pair of Identical Neurons: General Arguments. The phase locking of two identical and weakly coupled neurons can be easily investigated in the phase reduction framework. When the coupling between the neurons is symmetric, the two neurons are phase locked at large time with a phase shift ψ that satisfies

$$\Gamma^-(\psi) = \frac{1}{2} [\Gamma(\psi) - \Gamma(-\psi)] = 0 \quad (3.9)$$

Obviously $\psi = 0$ and $\psi = \pi$ are solutions; they correspond, respectively, to in-phase locking and anti-phase locking. Other zeros of Γ^- may also exist, that represent out-of-phase lockings. Only solutions that are stable with respect to small perturbations, i.e., that also satisfy the condition

$$\frac{d\Gamma^-}{d\psi}(\psi) < 0 \quad (3.10)$$

can be reached at large time.

We now investigate the stability of the in-phase solution for a reciprocal excitatory interaction ($V_{\text{syn}} \approx 0$). It is determined by the sign of

$$\frac{d\Gamma^-}{d\psi}(0) = \Gamma'(0) = -\frac{1}{2\pi} \int_0^{2\pi} \tilde{Z}(u) g'_{\text{syn}}(u) du \quad (3.11)$$

where $\tilde{Z}(u) = Z(u)$ for interactions described by equation 2.9 and $\tilde{Z} = Z(u)[V_{\text{syn}} - V(u)]$ when the interaction is given by equation 2.2.

3.2.1 Neurons with Type I Response. The simplest response of a neuron to depolarizing perturbations is to advance the firing of the next spike, outside its region of refractoriness. This corresponds to a response function Z of type I, nearly equal to 0 during the spike and the absolute refractory period, and positive on the rest of the limit cycle. The function \tilde{Z} has the same shape as Z up to a change of scale of the order of $V_{\text{syn}} - V_{\text{eq}}$ where V_{eq} is the potential of the neuron near rest (for interactions described by equation 2.2). This stems from the fact that the driving force $V_{\text{syn}} - V(u)$ does not vary much outside the refractory region. We plot in Figure 1a an example of a type I response function obtained for the model of Connor *et al.* while Figure 1b displays \tilde{Z} for the same model.

Let T_r denote the length of the refractory region. The only contribution to $\Gamma'(0)$ will come from the rest of the limit cycle where $\tilde{Z} > 0$. Therefore:

$$\Gamma'(0) = -\frac{1}{2\pi} \int_{\psi_r}^{2\pi} \tilde{Z}(u) g'_{\text{syn}}(u) d\psi \quad (3.12)$$

where $\psi_r = 2\pi T_r/T$ is the length of the refractory region expressed in terms of phase. Let us introduce $\psi^* = \max(\psi_r, \psi_p)$, where ψ_p is the phase at which g_{syn} reaches its peak value. We have then

$$\Gamma'(0) = -\frac{1}{2\pi} \int_{\psi_r}^{\psi^*} \tilde{Z}(u) g'_{\text{syn}}(u) d\psi - \frac{1}{2\pi} \int_{\psi^*}^{2\pi} \tilde{Z}(u) g'_{\text{syn}}(u) d\psi \quad (3.13)$$

The first contribution to $\Gamma'(0)$ is negative and tends to stabilize the in-phase state while the second is positive and tends to destabilize it. Therefore the stability of the in-phase locked state will depend on the balance between these two terms.

If $\psi_r > \psi_p$ the stabilizing term disappears. This provides a sufficient condition for the in-phase state to be unstable. This situation will be encountered, in particular, for interactions with a rise time short with respect to T_r . We can estimate in such cases how the instability rate depends on τ_1 and τ_2 (note that ψ_p varies slowly when τ_1 or τ_2 increases). At fixed τ_2 the overlap between \tilde{Z} and g' increases with τ_1 . Therefore $\Gamma'(0)$ increases also and the in-phase state becomes more unstable. Similarly, increasing τ_2 at fixed τ_1 enhances the instability of the in-phase state.

Another general statement, valid even if $\psi_p > \psi_r$, can be made if \tilde{Z} reaches its maximum just before the firing of the spike and then drops abruptly to 0 (as occurs for the Lopicque model, see below). In that

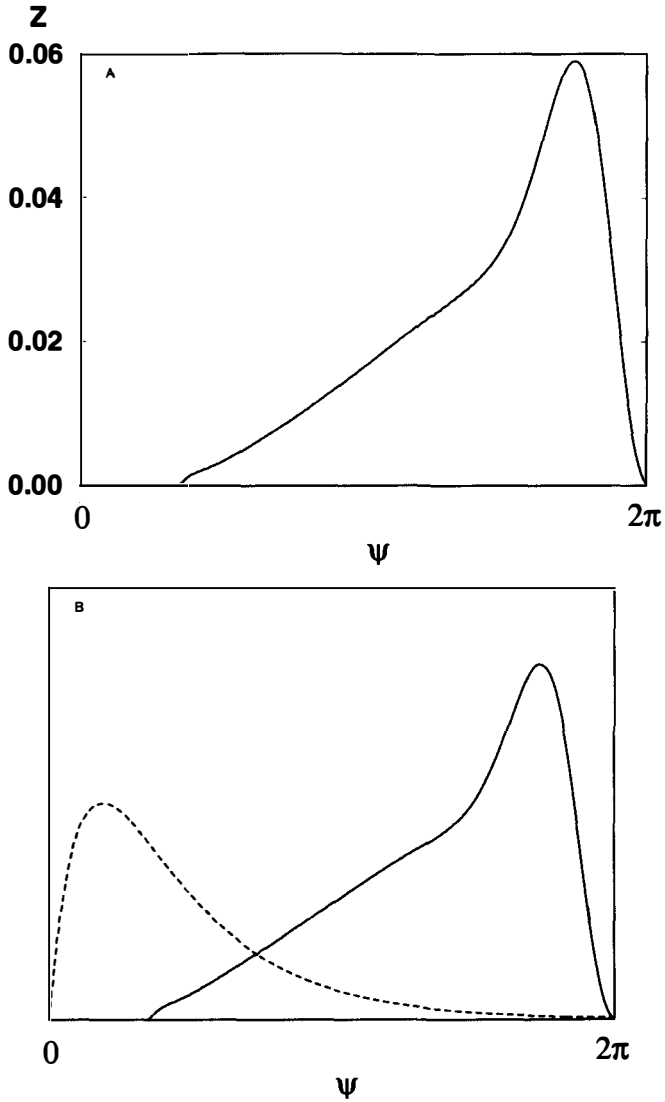


Figure 1: (a) The response function Z as a function of time along one cycle of the model of Connor *et al.* The frequency of the neuron is approximately 57 Hz. The origin of the time scale is set at the firing of the spike. (b) The two functions $-Z(\psi)[V(\psi) - V_{\text{syn}}]$ (solid line) and $g_{\text{syn}}(\psi)$ (dashed line) for the model of Connor *et al.* Same frequency as in (a). The scales for both curves are arbitrary. The interaction is excitatory ($V_{\text{syn}} = 0$). The rise time is $\tau_2 = 1$ msec and the decay time is $\tau_1 = 3$ msec. The convolution of these two functions yields the effective interaction Γ of the phase model.

case the excitation is always desynchronizing. Indeed, since the function $g_{\text{syn}}(\psi)$ is periodic one has

$$\int_0^{\psi_p} g'_{\text{syn}}(\psi) d\psi = - \int_{\psi_p}^{2\pi} g'_{\text{syn}}(\psi) d\psi \quad (3.14)$$

As $g'_{\text{syn}}(\psi) > 0$ in the interval $[0, \psi_p]$, the mean value theorem ensures that for some ψ_1^* in this interval

$$\frac{\int_0^{\psi_p} g'_{\text{syn}}(\psi) \tilde{Z}(\psi) d\psi}{\int_0^{\psi_p} g'_{\text{syn}}(\psi) d\psi} = \tilde{Z}(\psi_1^*) \quad (3.15)$$

Similarly there exists some ψ_2^* in the interval $[\psi_p, 2\pi]$ such that

$$\frac{\int_{\psi_p}^{2\pi} g'_{\text{syn}}(\psi) \tilde{Z}(\psi) d\psi}{\int_{\psi_p}^{2\pi} g'_{\text{syn}}(\psi) d\psi} = \tilde{Z}(\psi_2^*) \quad (3.16)$$

Using equation 3.14 and the fact that \tilde{Z} is monotonically increasing we have

$$\int_0^{\psi_p} g'_{\text{syn}}(\psi) \tilde{Z}(\psi) d\psi < - \int_{\psi_p}^{2\pi} g'_{\text{syn}}(\psi) \tilde{Z}(\psi) d\psi \quad (3.17)$$

Therefore the desynchronizing contribution to $\Gamma'(0)$ is predominant.

One can rely on a similar argument to prove that if \tilde{Z} is differentiable everywhere and has only one maximum, an excitatory interaction with instantaneous rise is desynchronizing whatever its decay time.¹

These results can be extended by continuity. It is clear that the two contributions to $\Gamma'(0)$ can be comparable only if ψ_p and the maximum ψ_m of \tilde{Z} are not too far apart. Since $\psi_p < \pi$, this implies that excitation can be synchronizing only if the resetting to 0 of \tilde{Z} is slow and both τ_1 and τ_2 are sufficiently large.

A condition that we have implicitly assumed here is that the interaction is not fast enough to take place almost totally in the refractory region ($Z \approx 0$). Indeed, in that case the effect of the interaction will be very small and no conclusion can be drawn from the present study.

Summarizing, we have shown that for neurons of type I an excitatory synaptic interaction is desynchronizing when the interaction is not too fast (so as not to occur entirely inside the refractory period) and when

¹If both the interaction and the response function are discontinuous at the time of the spike the linear stability analysis cannot be performed. If both discontinuities are finite, $\Gamma(\psi)$ is continuous at $\psi = 0$ but its derivative is discontinuous at that point. This situation occurs in the integrate-and-fire model investigated by Tsodyks *et al.* (1993). If the discontinuity of the interaction is infinite (δ function) the function Γ is discontinuous as occurs, for instance, in the model studied by Kuramoto (1991) and by Mirollo and Strogatz (1990). For these two models it has been shown (Kuramoto 1984; Mirollo and Strogatz 1990; Tsodyks *et al.* 1993) that excitation is synchronizing at any coupling strength. These results can also be proved in the weak coupling limit using phase reduction, although a linear stability analysis cannot be applied in these cases.

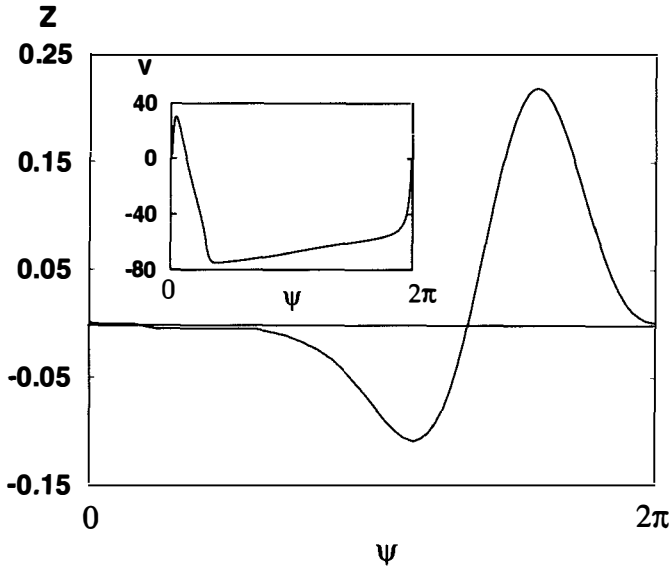


Figure 2: The response function Z along one cycle of the HH model. The frequency of the neuron is approximately 68 Hz. The inset shows the evolution of the membrane potential during the oscillation.

the peak of the synaptic interaction is located sufficiently before the peak of the response function. In particular, if the response function presents a steep decay after its maximum, excitation is desynchronizing in a very large domain (if not for all the values) of the synaptic parameters.

3.2.2 Neurons with Type II Response. Oscillatory neurons can respond to a small and instantaneous depolarization in some region of the limit cycle by delaying the firing of the next spike. In that part of the limit cycle, the function Z is then negative. The Hodgkin–Huxley model provides an example of such a response, as shown in Figure 2. Z displays a negative region after the refractory period. This negative response stems from the fact that in this region, a depolarization activates the delayed rectifier potassium current more than the sodium current, leading to a total hyperpolarizing current and a delay in the firing of the next spike.

In the following, such response functions will be called responses of type II. This classification of the responses into type I and type II does not exhaust a priori all the possibilities; other types of response might be encountered.

For response functions of type II, the argument given in the previous section no longer applies, because, even when the maximum of the synaptic interaction occurs inside the refractory region, there is a synchronizing contribution to $\Gamma'(0)$ coming from the region of negative response. If this negative region is large enough or if the interaction is sufficiently fast to occur mostly in that region the integral of equation 3.12 will be dominated by this synchronizing contribution and the in-phase state will be stable. On the other hand, the destabilizing contribution increases with the synaptic time constants τ_1 and τ_2 ; this can lead to a bifurcation to a state of out-of-phase locking for slower interactions.

3.3 Examples. Let us now see some examples to illustrate these general considerations.

The Lopicque model recalled in Section 2.2 is the simplest example of a model with type I response. More specifically

$$Z(\psi) = \frac{1}{I_{\text{ext}}} e^{\psi} \quad (3.18)$$

for $0 \leq \psi < 2\pi$; the constant I_{ext} being defined as in Section 2.2. If a refractory period is introduced Z has the above exponential profile outside the refractory region and is equal to 0 inside it. In view of the previous section, excitation is always desynchronizing at weak coupling for the Lopicque model. This can be checked by calculating the effective interaction Γ for that model. Indeed, performing the convolution integral between this function Z and the interaction (equations 3.4 and 3.5) according to equation 3.2 one finds

$$\Gamma(\psi) = K_1 \Gamma_1(t) - K_2 \Gamma_2(t) \quad (3.19)$$

where $t = T_0 \psi / 2\pi$ ranges from 0 to T_0 ,

$$K_j = \frac{gA}{I_{\text{ext}} T_0} \frac{1}{1 - 1/\tau_j} \frac{1}{1 - e^{-T_0/\tau_j}} \quad (3.20)$$

($j = 1, 2$) and the functions Γ_1 and Γ_2 are related to the two exponential terms of the interaction. Inside the refractory period ($0 \leq t \leq T_r$)

$$\Gamma_j(t) = e^{(t-T_r)/\tau_j} \left(e^{(T_0-T_r)(1-1/\tau_j)} - 1 \right) \quad (3.21)$$

and outside it

$$\Gamma_j(t) = e^{t-T_r} \left(e^{-T_0/\tau_j} - 1 \right) + e^{(t-T_0)/\tau_j} \left(e^{T_0-T_r} - e^{-T_r/\tau_j} \right) \quad (3.22)$$

Γ^- has, in addition to unstable in-phase and anti-phase solutions, a stable out-of-phase solution. At given τ_2 and T_r this out-of-phase solution increases with τ_1 until it reaches anti-phase at a critical value $\tau_1^c(T_0)$, as shown in Figure 3.

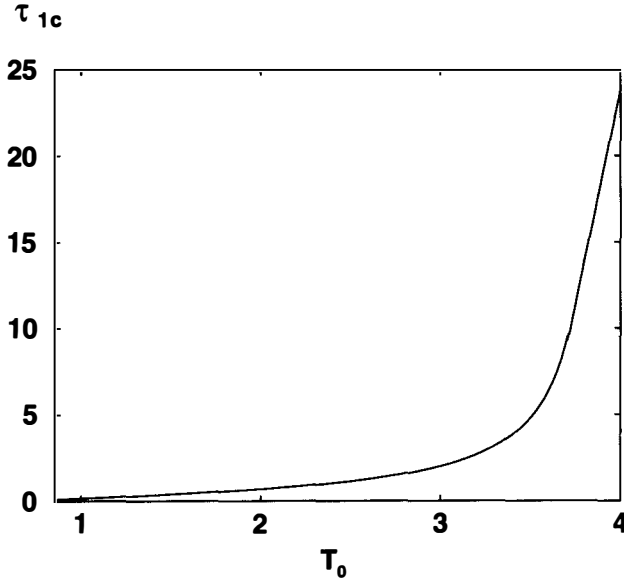


Figure 3: Critical decay time, τ_1^c at which the integrate-fire-model at weak coupling reaches anti-phase as a function of the natural period T_0 , for $\tau_2 = 0.1$ and $T_r = 0.3T$.

We now consider the model of Connor *et al.*, the response function of which is displayed in Figure 1 for a neuron oscillating with a period $T = 17.4$ msec ($\psi_r \approx 2\pi/5$). We have studied the phase locking of two symmetrically coupled neurons for different values of τ_1 and τ_2 and computed numerically the phase shift between the two neurons at weak coupling using the phase reduction method (evaluating equation 3.2 and solving equation 3.9). In all the cases studied the neurons lock out-of-phase, as can be seen in Figure 4. For a given τ_2 the phase shift increases with τ_1 . Anti-phase is reached at finite value of τ_1 . For example, anti-phase locking is found at $\tau_1 = 31$ msec for $\tau_2 = 0.5$ msec, $\tau_1 = 11.5$ msec, for $\tau_2 = 1$ msec, and $\tau_1 = 5$ msec for $\tau_2 = 2$ msec. Similarly the phase shift increases with τ_2 at given τ_1 . It is important to note that, even at very large τ_1 and τ_2 , the peak of the interaction occurs well before the peak of \tilde{Z} (see Fig. 1b where the peak of \tilde{Z} occurs well inside the second half of the oscillation). That is why excitation is always desynchronizing in this model.

This behavior is qualitatively independent of the frequency of the oscillations but at smaller frequencies longer synaptic times will be necessary to achieve a given phase shift. For instance, for a frequency of

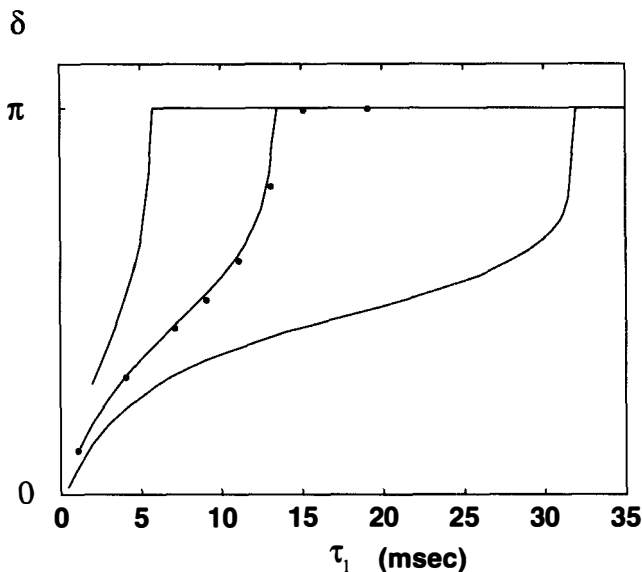


Figure 4: Dephasing δ between two coupled neurons (phase model derived from the model of Connor *et al.*) as a function of the decay time τ_1 for an excitatory interaction. Same frequency as in Figure 1. Three values of the rise time τ_2 are considered (curves from right to left): 0.5, 1, and 2 msec. Dots were obtained by integration of the full model for $\tau_2 = 1$ msec and $g = 0.05$ mS/cm² and show a very good agreement with the prediction of the phase model.

18 Hz and a rise time of $\tau_2 = 2$ msec the transition to anti-phase occurs at $\tau_1 \approx 9.1$ msec, which corresponds to $\psi_p = 1.04$.

As an example of type II response function we consider the HH model. This model has been studied in Hansel *et al.* (1993a,c) and here we simply summarize the results. In-phase synchronization of a pair of neurons is achieved for low firing rates or small synaptic time constants, because the condition mentioned above is satisfied: the negative part of the response function is large enough to dominate the integral of equation 3.12. When the period of the neurons decreases or the duration of the synaptic interaction increases, a pitchfork bifurcation to two symmetric stable out-of-phase states occurs. For a frequency of 68 Hz and a rise time $\tau_2 = 2$ msec the bifurcation takes place at $\tau_1^c \approx 5.1$ msec (Hansel *et al.* 1993c). For $\tau_2 = 0$ (instantaneous rise of the interaction) the bifurcation occurs at $\tau_1^c \approx 10$ msec. Beyond this bifurcation, in-phase synchrony is lost and excitation becomes desynchronizing. It is interesting to note

that this bifurcation occurs even for synaptic interactions that rise very fast. However, the bifurcation point τ_1^c is a decreasing function of τ_2 , as expected from the argument of the previous section.

Another interesting consequence of the negative response region is that the firing rate of a pair of identical HH neurons decreases when the coupling increases. This effect can be understood using phase models. The possibility of such a paradoxical reduction of the firing rate by excitatory coupling has been suggested in Kopell (1988). More details about this effect in the HH model can be found in Hansel *et al.* (1993a).

3.4 Large Networks. In this section we investigate the dynamics of large and fully connected excitatory networks neurons at weak coupling. We shall restrict ourselves to the model of Connor *et al.* and shall illustrate on this example the consequences of the out-of-phase locking of pairs of neurons on the collective properties of large networks. One expects intuitively that if in-phase locking is unstable for pairs of neurons, full synchrony will not be achieved in the network. This instability of the in-phase state is exemplified in Figure 5 for a network of 100 neurons when $g = 0.1$ mS/cm² (numerical integration of the equations for the full model). At time $t = 0$, the network is almost fully synchronized in-phase. This synchrony is destroyed at later times by the excitatory interactions as indicated by the dispersion of the firing times of the neurons [see also Pinsky (1994) for another example of instability of the fully synchronized state in a network of excitatory neurons]. It can be proved easily in the framework of phase reduction that for any network of excitatory neurons such an instability occurs if $\Gamma'(0) > 0$, whatever the connectivity.

In such situations the network is frustrated as any two neurons tend to lock with a phase shift $\psi \neq 0$ and these constraints cannot be all satisfied simultaneously. A large network then settles in a state of partial synchrony. Different types of partially coherent states may occur; in the framework of phase reduction they can be characterized by the nature (singular or continuous) of the one oscillator probability density $P(\phi, t)$ and its time dependence. These states can exhibit a large degeneracy. It is a major issue to determine which type of states occur generically. In the following we will give examples of partially coherent states that occur for the model of Connor *et al.* A more complete study of this issue is deferred to another paper (Monnet *et al.* 1994) where we will use phase reduction methods to show that these states should be generic in a broad class of models.

3.4.1 Rotating Wave States. Among the possible collective states of partial synchrony that can exist, an important and wide class consists of the so called "rotating waves." Such collective states have been introduced in Kuramoto (1991) and Watanabe and Strogatz (1993). They correspond

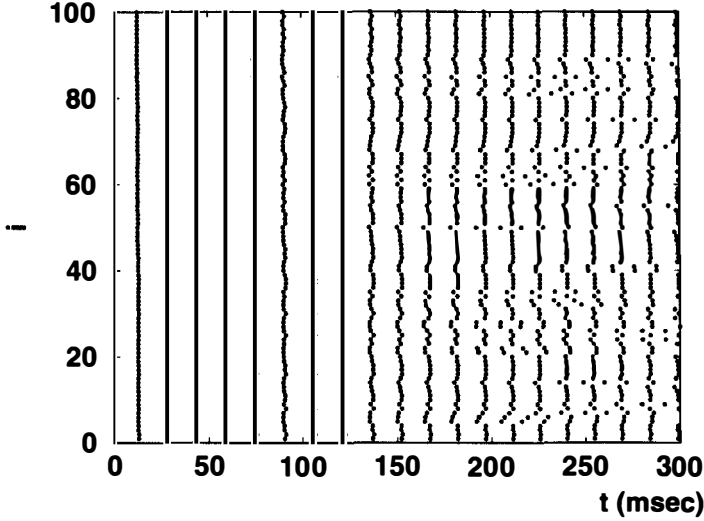


Figure 5: Firing times for a fully connected network of 100 neurons with excitatory interactions (model of Connor *et al.*, $\tau_1 = 3$ msec, $\tau_2 = 1$ msec, and $g = 0.1$ mS/cm²) presented as a raster-like display. Neurons were conventionally labeled from 1 to 100 (ordinate). Each dot corresponds to the firing of a spike by one neuron.

to a one phase probability distribution:

$$P(\psi, t) \equiv P(\psi - \Omega t) \quad (3.23)$$

that is continuous, even in the absence of noise, and is periodic in time with a frequency Ω . The distribution can be fully characterized by defining the order parameters ($n \geq 0$):

$$R_n(t) = \frac{1}{N} \sum_{k=1}^N e^{in\psi_k(t)} \quad (3.24)$$

In large networks, these quantities are the Fourier coefficients of the phase distribution at time t . The moduli of the R_n are constant in time and the dependence on time of their arguments is

$$\arg R_n = n\Omega t + \alpha_n \quad (3.25)$$

where the α_n are some constant phase shifts. The degree of phase coherence across the network can be measured by $|R_1|$. More generally, the

$|R_n|$ measure the tendency of the neurons to cluster into n subpopulations that spike coherently. Note that the fully synchronized state and the asynchronous state are particular forms of rotating waves. They correspond respectively to $R_n = 1$ for all n [distribution $P(\psi, t) = \delta(\psi - \Omega t)$] and $R_n = 0$ for all n [$P(\psi, t) = 1/2\pi$]. Note also that if only a finite number of Fourier modes are retained to describe the effective interaction, rotating waves can be written in terms of the same number of (complex) order parameters.

An example of rotating wave state (with frequency $\Omega \approx 62$ Hz) can be found in the phase model derived from the model of Connor *et al.* for $\tau_1 = 3$ msec and $\tau_2 = 2$ msec.² The firing pattern reached at large time is shown on Figure 6a for almost fully synchronized initial conditions. Similar patterns are obtained for other initial conditions (close to the asynchronous state or to a 2-cluster state). The time dependence of $|R_1|$ is plotted in Figure 7, showing that at large time the same value $|R_1| \approx 0.31$ is reached for the different initial conditions we considered. We have checked that the $|R_n|$ (up to $n = 4$) are also converging at large time to constant values that are the same for these three types of initial conditions. This final state has therefore a large basin of attraction. Another characteristic of this rotating wave is that cross-correlations of pairs of neurons display phase shifts that vary from pair to pair. These dephasings are a consequence of the frustration present in the network. Numerical integration of the full system of equations shows at large time a partially synchronized state, similar to the rotating wave of the phase model. This is illustrated on Figure 6b, where the firing pattern of a network of 100 neurons is displayed for the same set of parameters as above.

3.4.2 Cluster States and Switching States. In the previous section we saw that the system could overcome frustration by setting in a state with a continuum of dephasings (rotating wave). Conversely, the network may settle in cluster states, where groups of neurons display full synchrony. In an n -cluster state (Golomb *et al.* 1992; Kaneko 1990; Okuda 1993) the network breaks into n groups with a fraction p_i ($i = 1, \dots, n$) of the neurons in group i . In each group, all the neurons are locked in-phase. The different groups display nonzero phase shift that may depend on time. The distribution corresponding to this state is singular and can be written

$$P(\psi, t) = \sum_{i=1}^n p_i \delta[\psi - \psi_i(t) - \Omega t] \quad (3.26)$$

where the functions of time $\psi_i(t)$ are the positions of the clusters.

For 2-clusters the phase shift $\Delta_{12} = \psi_1(t) - \psi_2(t)$ between the two groups is constant in time. The linear stability analysis of a general 2-

²This model was obtained by truncating at order 4 the Fourier expansion of the interaction function Γ .

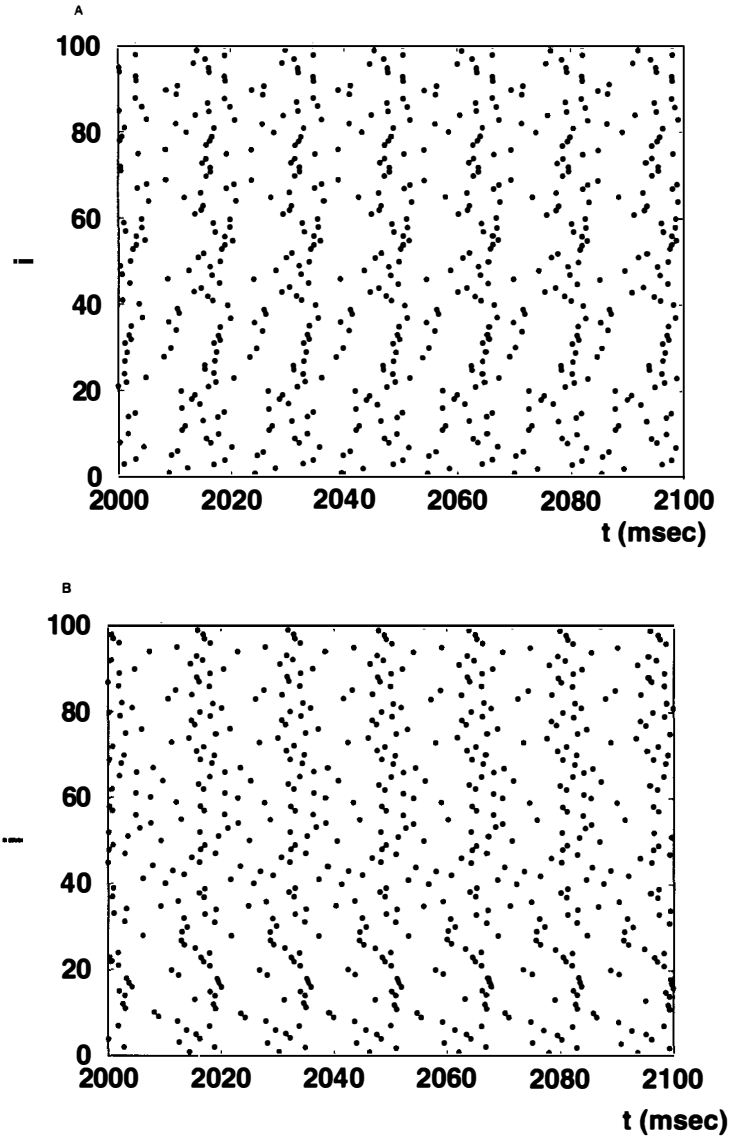


Figure 6: Firing times for a fully connected network of 100 neurons with excitatory interactions (model of Connor *et al.*, $\tau_1 = 3$ msec, $\tau_2 = 2$ msec, and $g = 0.1$ mS/cm²), starting from an almost synchronized initial condition. (a) For the phase model derived at weak coupling. (b) For the full model.

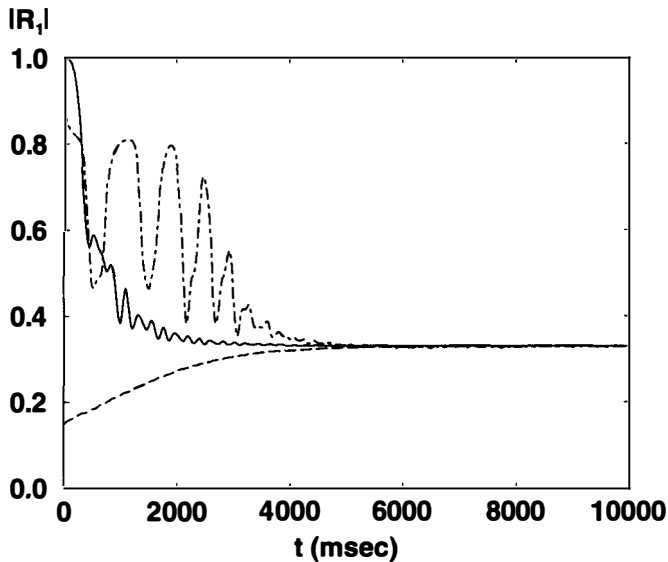


Figure 7: Absolute value of the first order parameter R_1 for the phase reduction of the model of Connor *et al.* Interaction is excitatory and characterized by $\tau_1 = 3$ msec and $\tau_2 = 2$ msec. Different initial conditions are considered: fully synchronized (solid line), random (dashed line), and two-cluster (dot-dashed line).

cluster state can be performed and the eigenvalues expressed in term of derivatives of Γ at 0 and $\pm\Delta_{12}$ (Hansel *et al.* 1993b; Okuda 1993).

For the model of Connor *et al.* random initial conditions lead to a rotating wave when $\tau_1 = 3$ msec and $\tau_2 = 1$ msec. However, for other initial conditions simulations show a rapid convergence to a 2-cluster state (Figure 8a). The same behavior is found for the corresponding phase model. A remarkable point is that the stability analysis of the 2-cluster states of the phase model reveals that they are linearly unstable. At first sight, it seems paradoxical that the dynamics may lead to an unstable state. However, similar phenomena have been observed for other networks of coupled neurons and have been explained in terms of heteroclinic loops between two 2-cluster states (Hansel *et al.* 1993b). It is then the pairs of connected 2-cluster states that constitute stable states. As in this previous work, adding a very small noise induces periodic switching between 2-cluster states, i.e., a quasiperiodic behavior of the network. Periodic switching also occurs in the full model, as illustrated

on Figure 8b. The order parameters R_n are not constant in time as they were for rotating wave states, but display oscillations with a period that depends logarithmically on the variance of the noise (Hansel *et al.* 1993b; Stone and Holmes 1991).

3.4.3 The Asynchronous State. When the frustration is too strong the network may set in a completely asynchronous stable state where the number of neurons spiking in a given time interval is constant in time. At weak coupling, this state always exists as can be shown in the framework of phase reduction. Expanding the effective phase interaction in Fourier modes:

$$\Gamma(\psi) = \sum_{m=0}^{\infty} a_m \cos(n\psi) + b_m \sin(n\psi) \quad (3.27)$$

it can be proved (Kuramoto 1984; Strogatz and Mirollo 1991) that the asynchronous state is stable iff $b_n > 0$ for all n . Note that the stability of the asynchronous state implies the stability of anti-phase locking for a pair of neurons; however, the converse is not true.

In the model of Connor *et al.* phase reduction predicts, for neurons spiking at 57 Hz and $\tau_2 = 2$ msec, that the asynchronous state becomes stable above $\tau_1 \approx 7.5$ msec. Numerical integration of the full system of nonlinear differential equations describing this network is in agreement with this prediction. This has been checked, for $\tau_1 = 8$ msec, $\tau_2 = 2$ msec ($t_p \approx 3.6$ msec), by comparing the time fluctuations of the average activity

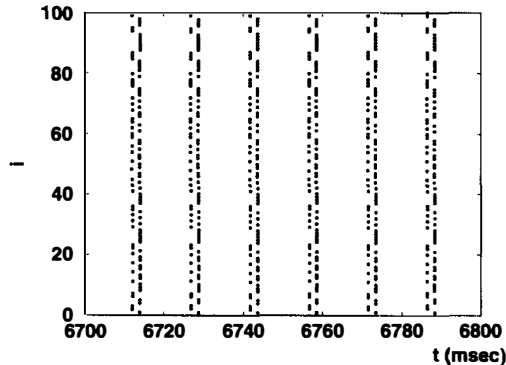


Figure 8: Firing times for a fully connected network of 100 neurons with excitatory interactions (model of Connor *et al.*, $\tau_1 = 3$ msec, $\tau_2 = 1$ msec, and $g = 0.1$ mS/cm²). (a) Without noise, for a random initial condition. *Continued next page.*

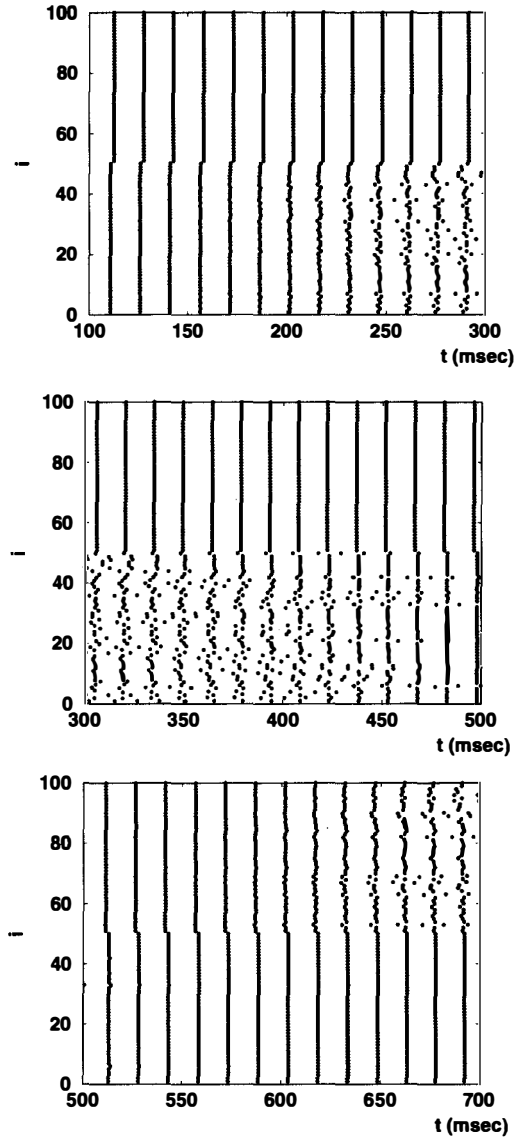


Figure 8: (b) With noise when the initial condition is a two-cluster state.

$\bar{S}(t)$ (i.e., the fraction of neurons emitting a spike at time t) for different sizes of the network. Indeed, our simulations show that the fluctuations decay to zero like $1/\sqrt{N}$ as expected in the asynchronous state.

4 Beyond Weak Coupling

In this section we investigate the phase locking of a pair of identical excitatory neurons with response of type I, without restricting ourselves to the weak coupling limit. We examine whether in-phase locking can be recovered at high coupling. This could be due to amplitude effects, or phase effects that lie beyond the averaging framework of phase reduction. We first investigate analytically an integrate-and-fire model in which amplitude effects are totally absent. Then we consider the model of Connor *et al.* that displays both phase and amplitude effects.

4.1 Integrate and Fire Neurons. This model is actually a pure phase model due to the absence of amplitude effects, but it is only at weak coupling that the interaction between neurons is a function of the phase difference. However, this simple model can be studied analytically at any coupling. We shall present here the results obtained when no refractory period is taken into account and, for the sake of conciseness, we shall just give an outline of the computations involved.

At coupling g , two identical integrate-and-fire neurons converge to a phase locked state characterized by a firing period $T(g)$ and a time shift δ between the firing times of neuron 1 and neuron 2. Integrating the dynamics over one cycle, the periodicity condition leads to two equations that determine T and δ ($\tau_0 = 1$):

$$I_{\text{ext}}(1 - e^{-T}) + e^{-T} \int_0^T e^t g_1(t) dt = \theta \quad (4.1)$$

$$I_{\text{ext}}(1 - e^{-T}) + e^{\delta-T} \int_{-\delta}^{T-\delta} e^t g_2(t) dt = \theta \quad (4.2)$$

where

$$g_1(t) = \begin{cases} gA \left(\frac{e^{-(t+\delta)/\tau_1}}{1 - e^{-T/\tau_1}} - \frac{e^{-(t+\delta)/\tau_2}}{1 - e^{-T/\tau_2}} \right) & 0 \leq t < T - \delta \\ gA \left(\frac{e^{-(t+\delta-T)/\tau_1}}{1 - e^{-T/\tau_1}} - \frac{e^{-(t+\delta-T)/\tau_2}}{1 - e^{-T/\tau_2}} \right) & T - \delta \leq t < T \end{cases} \quad (4.3)$$

$$g_2(t) = \begin{cases} gA \left(\frac{e^{-(t+T)/\tau_1}}{1 - e^{-T/\tau_1}} - \frac{e^{-(t+T)/\tau_2}}{1 - e^{-T/\tau_2}} \right) & -\delta \leq t < 0 \\ gA \left(\frac{e^{-t/\tau_1}}{1 - e^{-T/\tau_1}} - \frac{e^{-t/\tau_2}}{1 - e^{-T/\tau_2}} \right) & 0 \leq t < T - \delta \end{cases} \quad (4.4)$$

We display in Figure 9 the numerical solution of these equations for $\tau_1 = 0.3$, $\tau_2 = 0.1$, $\theta = 1$, $I_{\text{ext}} = 1.1$ (the period for the uncoupled neurons is then $T_0 = 2.4$). Besides the two trivial solutions $\delta = 0$ and $\delta = T/2$ an out-of-phase solution exists. The corresponding phase shift starts at $g = 0$

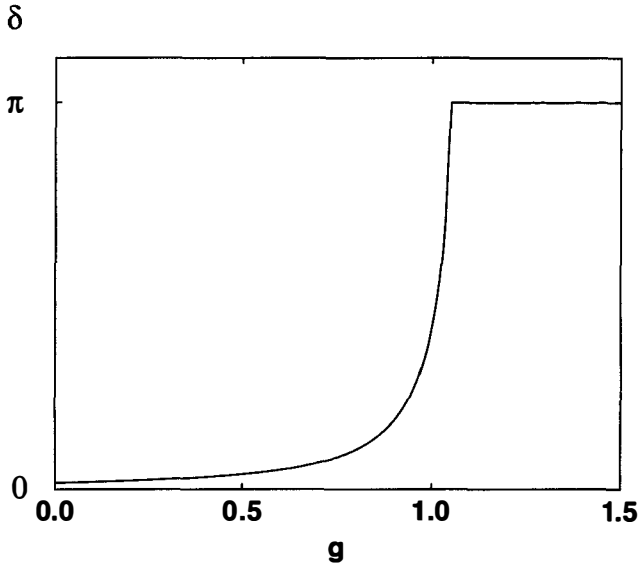


Figure 9: Dephasing as a function of the coupling for a pair of integrate-and-fire models in mutual excitatory interaction ($\tau_1/\tau_0 = 0.3$ and $\tau_2/\tau_0 = 0.1$).

from a finite value and increases with the coupling strength; anti-phase is reached at a finite value: $g \simeq 1.05$.

The stability of these different solutions can be investigated in the following way. Since the synaptic response is the difference of two exponentials, the interaction term $g_1(t)$ satisfies the second order differential equation:

$$\frac{d^2 g_1}{dt^2} + \alpha \frac{dg_1}{dt} + \beta g_1 = gA \sum \delta(t - t_{\text{spike}}) \quad (4.5)$$

where $\alpha = 1/\tau_1 + 1/\tau_2$, $\beta = 1/\tau_1\tau_2$, and the summation on the right-hand side is performed over all the spikes emitted by neuron 2 at times t_{spikes} prior to t . The dynamics of neuron 1 can then be rewritten as

$$\frac{dV}{dt} = -V + I_{\text{ext}} + g_1 \quad (4.6)$$

$$\frac{dg_1}{dt} = -\frac{g_1}{\tau_2} + z_1 \quad (4.7)$$

$$\frac{dz_1}{dt} = -\frac{z_1}{\tau_1} + gA \sum \delta(t - t_{\text{spike}}) \quad (4.8)$$

and we can do likewise for neuron 2. The interactions between the neurons are thus embodied in variables g_i and z_i that are local in time. We can then derive, by integrating these equations, a six-dimensional mapping that associates to the p th spiking times $t_p^{(1)}$ and $t_p^{(2)}$ of neurons 1 and 2 and the values of the variables $g_1, z_1, g_2,$ and z_2 at those times, the next spiking times $t_{p+1}^{(1)}$ and $t_{p+1}^{(2)}$, and the values of the g_i and z_i at those later times. Periodic solutions of the dynamics are fixed points of this mapping and their linear stability can be investigated by linearizing the mapping. Due to the global time invariance of the system, 1 is always an eigenvalue. If all the other eigenvalues are of modulus smaller than 1, the solution is linearly stable; otherwise it is unstable.

Applying this method to the present case shows that for $g > 0$ the in-phase state is unstable on its whole domain of existence [it disappears, as well as the anti-phase state, at $g \simeq 1.93$ where the period $T(g)$ vanishes]. The intermediate solution is always stable and the anti-phase state is unstable at low g and becomes stable when it merges with the intermediate solution. Qualitatively similar results were found for all the values of τ_1 and τ_2 we have considered. The in-phase locked state was always unstable and a stable anti-phase state was achieved at large but finite g .

In a recent work van Vreeswijk *et al.* (1994) studied the Lapicque model when the time course of the synapse is described by an α function. This is a special case of the interaction we have used. Their conclusion is that excitation is desynchronizing in agreement with our results.

As a consequence, a large network of excitatory integrate-and-fire neurons cannot synchronize in-phase even at finite coupling strength [except if the interaction is instantaneous (Mirolo and Strogatz 1990)]. This fact was also found by Tsodyks *et al.* (1993) and the stability of the asynchronous state that may then arise was recently examined (Abbott and van Vreeswijk 1993; Treves 1993). Note also that at high coupling (T small) and given $\tau_1 = 0.3$ the in-phase solution remains unstable even for very small values of τ_2 (a real eigenvalue is larger than 1); this was checked for τ_2 as small as 10^{-3} . Therefore even a very fast rise of the interaction cannot stabilize in-phase synchronization.

4.2 The Model of Connor *et al.* For the model of Connor *et al.*, at large coupling strength, the phase shift between two neurons depends drastically on the synaptic time course. This is illustrated in Figure 10, for a fixed decay time constant $\tau_1 = 3$ msec. The results are qualitatively different depending on the value of the rise time τ_2 . For $\tau_2 = 1$ msec, the system locks in phase above 2.6 mS/cm² but for $\tau_2 = 2$ msec the phase shift between the two neurons increases and anti-phase is reached at $g \approx 1.3$ mS/cm². This behavior is similar to what we have found above for the integrate-and-fire model. In the first case, large networks are expected to synchronize in phase at high coupling. This is confirmed by simulations: for g above 2.6 mS/cm² full synchrony is achieved at a time

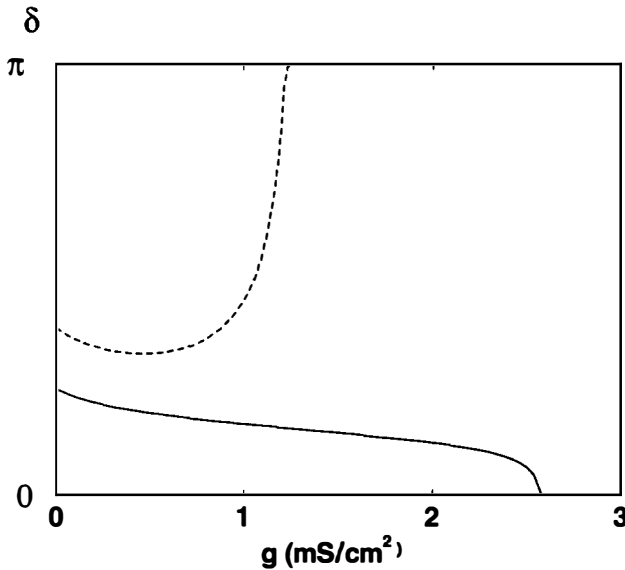


Figure 10: Dephasing δ , for the model of Connor *et al.*, as a function of the coupling for a pair of excitatory neurons. Here $\tau_1 = 3$ msec, while $\tau_2 = 2$ msec (dashed line) or $\tau_2 = 1$ msec (solid line).

of the order of 100 msec. In contrast, for $\tau_2 = 2$ msec and $g = 1.3$ mS/cm² the system stabilizes in a symmetric three-cluster state. In this state the network is broken into three similar groups of neurons. In each group all the neurons are locked in-phase while the phase shift between the clusters is $T/3$. Note that a stability analysis grounded on phase reduction reveals that this state is unstable at weak coupling. Clustering has also been found recently in models of thalamic (Golomb and Rinzel 1994; Golomb *et al.* 1994). In the present model it is found only in the strong coupling regime.

5 Conclusion

It has been proposed in Kopell (1988) that synaptic interactions should be classified as synchronizing or desynchronizing rather than excitatory or inhibitory when dealing with synchronization in systems of neurons. The results of the present work support this point of view since we have shown that the time course of the synaptic interaction plays a role as significant as its excitatory or inhibitory nature. To understand collec-

tive states of neural systems, one cannot separate the synaptic properties from cellular properties. This stands out clearly in our study, since the synchronizing effect of excitation was shown to depend on the response of the neurons to perturbations.

The main result of this work is the fact that for neurons with type I response, excitation is desynchronizing in a large range of synaptic parameters that includes physiologically realistic values. Even if the synaptic times are very short the interaction is desynchronizing for this type of neuron. In contrast, for neurons of type II sufficiently fast excitation can be synchronizing. These results have been based on general arguments valid at weak coupling. The study of specific examples has allowed us to extend it to intermediate values and even in some cases to strong values of the coupling strength. We have also given examples of some of the consequences of these results for the dynamics of a large network of identical excitatory neurons. The trend of the neurons to lock out-of-phase induces frustration in the network that settles then in *partially* coherent states, such as rotating wave states. An important characteristic of these rotating waves is that the activities of the neurons are then correlated with phase shifts. When the frustration effects in the network become too strong, a transition to the completely asynchronous state can take place in spite of the homogeneity of the network and the absence of external noise.

In this paper we have focused on excitatory interactions. However, the reduction to phase models can also be used for predicting the effect of inhibitory synapses. For neurons of type I, one can show that under very general conditions inhibition can be synchronizing, leading to a bistability where both the in-phase locked state and the anti-phase locked state of a pair of identical inhibitory neurons are stable. If this synchronizing effect is sufficiently strong (for instance for fast synapses), the anti-phase can even lose stability and the in-phase state is then the only stable state of locking. Similar results have been found for an integrate-and-fire model in van Vreeswijk *et al.* (1994). A more systematic study of this effect and its consequences for large networks will be published elsewhere (Hansel *et al.* 1994).

We have considered only large homogeneous and fully connected networks. An important issue is to assess the effect of the heterogeneities found in biological situations: dispersion of neural characteristics (membrane time constant, ionic conductances etc.), various sources of noise, connectivity pattern. It would be very interesting to determine whether these can counterbalance to some extent the desynchronizing effect of excitation by effectively reducing the frustration in the system (Hansel and Mato 1993; Tsodyks *et al.* 1993). This would give some insight on the ubiquity of partially coherent states and phase shifts in cross-correlations for biological systems.

Finally let us remark that response functions are amenable to experiments (Reyes and Fetz 1993a,b). It would be very interesting to determine

the responses of neurons in biological systems where collective effects have been observed. Are type I responses representative? If not, this would, for instance, question the relevance of integrate-and-fire models for modeling such systems. In particular, such observations would be very interesting for central pattern generators (CPGs). Can synchronization properties in such systems be related to the response function of the neurons? One may also wonder whether the type of response can be modified by neuromodulatory effects leading to different patterns of synchrony. If so, this could have consequences from the functional point of view.

Appendix

The Hodgkin–Huxley Model. The HH model provides the simplest framework to describe spike generation in a real biological situation, namely the squid's giant axon. An HH neuron is described by a set of four variables $\mathbf{X} = (V, m, h, n)$ where V is the membrane potential, m and h the activation and inactivation variables of the sodium current, and n the activation variable of the potassium current. The corresponding equations read (Hodgkin and Huxley 1952):

$$C \frac{dV}{dt} = I - g_{\text{Na}} m^3 h (V - V_{\text{Na}}) - g_{\text{K}} n^4 (V - V_{\text{K}}) - g_{\text{l}} (V - V_{\text{l}}) \quad (\text{A.1})$$

$$\frac{dm}{dt} = \frac{m_{\infty}(V) - m}{\tau_m(V)} \quad (\text{A.2})$$

$$\frac{dh}{dt} = \frac{h_{\infty}(V) - h}{\tau_h(V)} \quad (\text{A.3})$$

$$\frac{dn}{dt} = \frac{n_{\infty}(V) - n}{\tau_n(V)} \quad (\text{A.4})$$

I is the external current injected into the neuron. It determines the neuron's firing rate. The parameters g_{Na} , g_{K} , and g_{l} are the maximum conductances per surface unit for the sodium, potassium, and leak currents, V_{Na} , V_{K} , and V_{l} are the corresponding reversal potentials, and C is the capacitance per surface unit. For the squid's axon typical values of the parameters (at 6.3°C) are $V_{\text{Na}} = 50$ mV, $V_{\text{K}} = -77$ mV, $V_{\text{l}} = -54.4$ mV, $g_{\text{Na}} = 120$ mS/cm², $g_{\text{K}} = 36$ mS/cm², $g_{\text{l}} = 0.3$ mS/cm², and $C = 1$ μF/cm². The functions $m_{\infty}(V)$, $h_{\infty}(V)$, and $n_{\infty}(V)$ and the characteristic times (in milliseconds) τ_m , τ_n , τ_h , are given by $x_{\infty}(V) = a_x / (a_x + b_x)$, $\tau_x = 1 / (a_x + b_x)$ with $x = m, n, h$ and $a_m = 0.1(V + 40) / \{1 - \exp[(-V - 40)/10]\}$, $b_m = 4 \exp[(-V - 65)/18]$, $a_h = 0.07 \exp[(-V - 65)/20]$, $b_h = 1 / \{1 + \exp[(-V - 35)/10]\}$, $a_n = 0.01(V + 55) / \{1 - \exp[(-V - 55)/10]\}$, $b_n = 0.125 \exp[(-V - 65)/80]$.

For small values of I the system reaches a stable fixed point ($V_{\text{eq}} = -65$ mV for $I = 0$ μA/cm²). At $I_1 = 9.78$ μA/cm² the system undergoes an inverted Hopf bifurcation to the spiking regime. This behavior agrees

with the electrophysiological observation on the squid's axon that the oscillations start with finite amplitude and frequency. The periodic emission of spikes stops at $I_2 = 154.5 \mu\text{A}/\text{cm}^2$, where the fixed point becomes again stable.

The Model of Connor *et al.* The model of Connor *et al.* (1977) incorporates, in addition to the sodium and delayed rectifier potassium currents of the HH model, an A current and displays a much wider range of firing frequency than the Hodgkin–Huxley model. It is well known that the firing rates (from 50 to 120 Hz) that are achieved by the Hodgkin–Huxley model with usual parameters are much higher than is commonly observed in other preparations. On the basis of numerous observations, the so-called A current is often considered to widen the frequency range. Indeed this potassium current is characterized by an inactivation that is much slower than its activation and it will play a major role when one tries to depolarize a neuron starting from a situation of hyperpolarization. The slow deinactivation of the inward A current will then tend to impede fast membrane depolarization and firing rates ranging from 0 to 300 Hz are thus obtained in the model of Connor *et al.* with a linear current–frequency relation at low frequencies. The role of the A current in low frequency spiking was recently investigated in detail by Rush and Rinzel (1994).

The parameterizations of the sodium and delayed rectifier potassium currents for the HH model and the model of Connor *et al.* are very similar. Parameters for these currents are $V_{\text{Na}} = 55 \text{ mV}$, $V_{\text{K}} = -72 \text{ mV}$, $V_l = -17 \text{ mV}$, $g_{\text{Na}} = 120 \text{ mS}/\text{cm}^2$, $g_{\text{K}} = 20 \text{ mS}/\text{cm}^2$, $g_l = 0.3 \text{ mS}/\text{cm}^2$, and $C = 1 \mu\text{F}/\text{cm}^2$. $x_{\infty}(V) = a_x/(a_x + b_x)$, $\tau_x = 1/(a_x + b_x)$ with $x = m, n, h$ and $a_m = 0.1(V + 29.7)/\{1 - \exp[(-V - 29.7)/10]\}$, $b_m = 4 \exp[(-V - 54.7)/18]$, $a_h = 0.07 \exp[(-V - 48)/20]$, $b_h = 1/\{1 + \exp[(-V - 18)/10]\}$, $a_n = 0.01(V + 46.7)/\{1 - \exp[(-V - 46.7)/10]\}$, $b_n = 0.125 \exp[(-V - 56.7)/80]$. The A current is described in a similar way:

$$I_A = -g_A(V - V_A)A^3B \quad (5.1)$$

$$\frac{dA}{dt} = \frac{A_{\infty}(V) - A}{\tau_A(V)} \quad (5.2)$$

$$\frac{dB}{dt} = \frac{B_{\infty}(V) - B}{\tau_B(V)} \quad (5.3)$$

where

$$A_{\infty}(V) = 0.0761 \left[\frac{\exp[(V + 94.22)/31.84]}{1 + \exp[(V + 1.17)/28.93]} \right]^{1/3} \quad (5.4)$$

$$\tau_A(V) = 0.3632 + \frac{1.158}{1 + \exp[(V + 55.96)/20.12]} \quad (5.5)$$

$$B_{\infty}(V) = \frac{1}{[1 + \exp[(V + 53.3)/14.54]]^4} \quad (5.6)$$

$$\tau_B(V) = 1.24 + \frac{2.678}{1 + \exp[(V + 50)/16.027]} \quad (5.7)$$

The reversal potential $V_A = -75$ mV is slightly different from V_K and the conductance g_A is set here to 47.7 mS/cm². The only difference with the parameterization of Connor *et al.* (1977) is that we did not introduce the temperature scaling factor in the kinetics of activation and inactivation variables.

Acknowledgments

We are thankful to H. Sompolinsky and M. Tsodyks for most helpful discussions. We are indebted to D. Golomb, M.-L. Monnet, S. Seung, and H. Sompolinsky for careful and critical reading of the manuscript. D.H. acknowledges hospitality of the Center for Neural Computation and the Racah Institute of Physics of the Hebrew University. This work was partially supported by a Projet Concerté de Coopération Scientifique of Ministère des Affaires Étrangères. Part of the simulations were performed on the CRAY-C98 of IDRIS. While we were completing this paper we learned about the related work of C. van Vreeswijk *et al.* (1994). We thank B. Ermentrout for having brought it to our attention.

References

- Abbott, L. F., and van Vreeswijk, C. 1993. Asynchronous states in networks of pulse-coupled oscillators. *Phys. Rev.* **E48**, 1483–1490.
- Bush, P., and Douglas, R. 1991. Synchronization of bursting action potential discharge in a model network of neocortical neurons. *Neural Comp.* **3**, 19–30.
- Connor, J. A., Walter, D., and McKown, R. 1977. Neural repetitive firing: modifications of the Hodgkin-Huxley axon suggested by experimental results from crustacean axons. *Biophys. J.* **18**, 81–102.
- Ermentrout, G. B., and Kopell, N. 1984. Frequency plateaus in a chain of weakly coupled oscillators, I. *SIAM J. Math. Anal.* **15**, 215–237.
- Ermentrout, G. B., and Kopell, N. 1991. Multiple pulse interactions and averaging in systems of coupled neural oscillators. *J. Math. Biol.* **29**, 195–217.
- Golomb, D., and Rinzel, J. 1994. Clustering in globally coupled inhibitory neurons. *Physica* **D71**, 259–282.
- Golomb, D., Hansel, D., Shraiman, B., and Sompolinsky, H. 1992. Clustering in globally coupled phase oscillators. *Phys. Rev.* **A45**, 3516–3530.
- Golomb, D., Wang, X. J., and Rinzel, J. 1994. Synchronization properties of spindle oscillations in a thalamic reticular nucleus model. *J. Neurophysiol.* **72**, 1109–1126.
- Grannan, E. R., Kleinfeld, D., and Sompolinsky, H. 1992. Stimulus-dependent synchronization of neuronal assemblies. *Neural Comp.* **4**, 550–569.

- Hansel, D., and Mato, G. 1993. Patterns of synchrony in a heterogeneous Hodgkin-Huxley neural network with weak coupling. *Physica* **A200**, 662–669.
- Hansel, D., Mato, G., and Meunier, C. 1993a. Phase dynamics for weakly coupled Hodgkin-Huxley neurons. *Europhys. Lett.* **23**, 367–372.
- Hansel, D., Mato, G., and Meunier, C. 1993b. Clustering and slow switching in globally coupled phase oscillators. *Phys. Rev.* **E48**, 3470–3477.
- Hansel, D., Mato, G., and Meunier, C. 1993c. Phase reduction and neural modeling. In *Functional Analysis of the Brain Based on Multiple-Site Recordings, October 1992. Concepts Neurosci.* **4**, 192–210.
- Hansel, D., Mato, G., and Meunier, C. 1994. In preparation.
- Hodgkin, A. L., and Huxley, A. F. 1952. A quantitative description of membrane current and its application to conduction and excitation in nerve. *J. Physiol. (London)* **117**, 500–544.
- Kaneko, K. 1990. Clustering, coding, switching, hierarchical ordering and control in a network of chaotic elements. *Physica* **D41**, 136–172.
- Kopell, N. 1988. Toward a theory of modeling central pattern generators. In *Neural Control of Rhythmic Movements in Vertebrates*, A. Cohen, ed., pp. 369–413. John Wiley, New York.
- Kuramoto, Y. 1984. *Chemical Oscillations, Waves and Turbulence*. Springer, New York.
- Kuramoto, Y. 1991. Collective synchronization of pulse-coupled oscillators and excitable units. *Physica* **D50**, 15–30.
- Mirollo, R. E., and Strogatz, S. H. 1990. Synchronization of pulse-coupled biological oscillators. *SIAM J. Appl. Math.* **6**, 1645–1657.
- Monnet, M.-L., Hansel, D., Mato, G., and Meunier, C. 1994. In preparation.
- Neu, J. 1979. Coupled chemical oscillators. *SIAM J. Appl. Math.* **37**, 307–315.
- Okuda, K. 1993. Variety and generality of clustering in globally coupled oscillators. *Physica* **D63**, 424–436.
- Pinsky, P. 1994. Mathematical models of hippocampal neurons and neural networks: Exploiting multiple time scales. Ph.D. thesis, University of Maryland.
- Reyes, A. D., and Fetz, E. E. 1993a. Two modes of interspike interval shortening by brief transient depolarizations in cat neocortical neurons. *J. Neurophysiol.* **69**, 1661–1672.
- Reyes, A. D., and Fetz, E. E. 1993b. Effects of transient depolarizing potentials on the firing rate of cat neocortical neurons. *J. Neurophysiol.* **69**, 1673–1683.
- Rogawski, M. A. 1985. The A-current: How ubiquitous a feature of excitable cells is it? *TINS* **63**, 214–219.
- Rush, M. E., and Rinzel, J. 1994. The potassium A-current, low firing rates and rebound excitation in Hodgkin-Huxley models. Preprint.
- Stone, E., and Holmes, P. 1991. Unstable fixed points, heteroclinic cycles and exponential tails in turbulence production. *Phys. Lett.* **A155**, 29–42.
- Strogatz, S. H., and Mirollo, R. E. 1991. Stability of incoherence in a population of coupled oscillators. *J. Stat. Phys.* **63**, 613–635.
- Traub, R., and Miles, R. 1991. *Neuronal Networks of Hippocampus*. Cambridge University Press, New York.

- Treves, A. 1993. Mean field analysis of neuronal spike dynamics. *Network* **4**, 259–284.
- Tsodyks, M., Mitkov, I., and Sompolinsky, H. 1993. Patterns of synchrony in integrate and fire network. *Phys. Rev. Lett.* **71**, 1280–1283.
- Tuckwell, H. C. 1988. *Introduction to Theoretical Neurobiology*. Cambridge University Press, New York.
- Watanabe, S., and Strogatz, S. H. 1993. Integrability of a globally coupled oscillator array. *Phys. Rev. Lett.* **70**, 2391–2394.
- van Vreeswijk, C., Abbott, L. F., and Ermentrout, G. B. 1994. When inhibition not excitation synchronizes neural firing. *J. Comp. Neurosci.*, submitted.